Letters

A Two-Plate Capacitive Wireless Power Transfer System for Electric Vehicle Charging Applications

Fei Lu, *Student Member, IEEE*, Hua Zhang, *Student Member, IEEE*, and Chris Mi, *Fellow, IEEE*

***Abstract*—This letter proposes a two-plate capacitive wireless power transfer (CPT) system for electric vehicle charging applications. The vehicle chassis and the earth ground are used to transfer power, which can replace two plates in a conventional four-plate CPT system. Therefore, only two external plates are required in the proposed CPT system. The coupling capacitance between the plates allows the current to flow forward to the vehicle side, and the stray capacitance between the chassis and the earth ground provides the current-returning path. After analyzing the working principle of a CPT system, it shows that the voltage on the vehicle chassis can be reduced through switching frequency, the coupler structure design, and the compensation circuit design. Then, a downsized prototype is implemented to validate the proposed system, in which two inductors are used to compensate the capacitive coupler. Experimental results show that the prototype achieves 350-W power transfer with 74.1% dc–dc efficiency over an air-gap distance of 110 mm, and the RMS voltage on vehicle chassis is limited to 132 V.**

***Index Terms*—Capacitive power transfer, earth ground, low-voltage stress, two plates, vehicle chassis.**

I. Introduction

Capacitive power transfer (CPT) is a promising technology to achieve wireless power transfer [1]. It utilizes high-frequency electric fields to transfer power, which can also be called electrical resonance [2]. In recent years, different circuit topologies [3]–[6] have been proposed to realize both short- and long-distance CPT systems and promote the practical applications.

Conventionally, a CPT system utilizes four metal plates, horizontally [4] or vertically [7] arranged, forming two capacitive couplers to transfer power. Two plates are installed on the primary side as a transmitter, and the other two plates are at the secondary side as a receiver. There are coupling capacitances between plates, allowing the displacement currents to flow through.

To simplify the capacitive coupler structure in vehicle charging applications, this letter proposes a two-plate CPT system. The vehicle chassis and the earth ground work as two plates in the conventional four-plate CPT system. Therefore, only two external plates are required. The stray capacitance between the chassis and the ground is used as the current-flowing path, resulting in a compact system structure.

In this proposed CPT system, the voltage on the vehicle chassis should be reduced for safe operation. According to IEEE C95.1 standard [8], the RMS current flowing through human body is required to be smaller than 16.7 mA from 100 kHz to 110 MHz. Considering that the human resistance is about 500 Ω at high frequency [9], the allowed maximum RMS voltage on vehicle chassis is about 8.35 V in the worst case. This letter proposes three methods to reduce chassis voltage: increasing switching frequency, designing the coupler structure, and optimizing the compensation circuit.

In the electric vehicle charging application, it proves that when the system switches at 6.78 MHz and the compensation circuit is well designed, the chassis voltage can be limited to 8.35 V with 3.0-kW system power. A downsized prototype is implemented to validate the proposed system. Experimental results show that the RMS value of chassis voltage is limited to 132 V in a 1.0 MHz and 350-W system. In the future work, the voltage will be further reduced to a safe level.

II. System Working Principle

A. System Structure

The structure of a two-plate CPT system for electric vehicle charging applications is shown in Fig. 1.

On the primary side, an inverter is used to provide an ac excitation, followed by a compensation circuit. The earth ground P_1 and a metal plate P_2 work as the transmitter, and there is an insulation layer between them.

The parasitic capacitance between the vehicle chassis and the earth ground is used as the current returning path. In practical applications, the earth ground can also be connected with a metal plate to further reduce the conductive loss. It needs to be emphasized that this ground-side plate is optional. If it is used, it should have a good connection with the earth ground. For

Manuscript received May 16, 2017; revised June 14, 2017 and July 14, 2017; accepted July 29, 2017. Date of publication August 2, 2017; date of current version November 2, 2017. This work was supported in part by US Department of Energy Graduate Automotive Technology Education Grant and San Diego State University. Recommended for publication by Associate Editor Henry S. H. Chung. *(Corresponding author: Chris Mi.)*

The authors are with the Department of Electrical and Computer Engineering, San Diego State University, San Diego, CA 92182 USA (e-mail: feilu@umich.edu; hzhang@mail.sdsu.edu; cmi@sdsu.edu).

Color versions of one or more of the figures in this letter are available online at http://ieeexplore.ieee.org.

Digital Object Identifier 10.1109/TPEL.2017.2735365

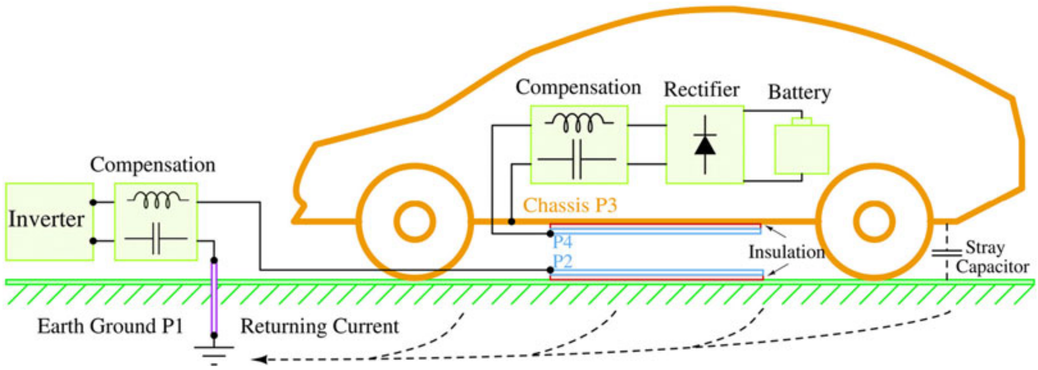

Fig. 1. Structure of a two-plate compact CPT system for electric vehicle charging applications.

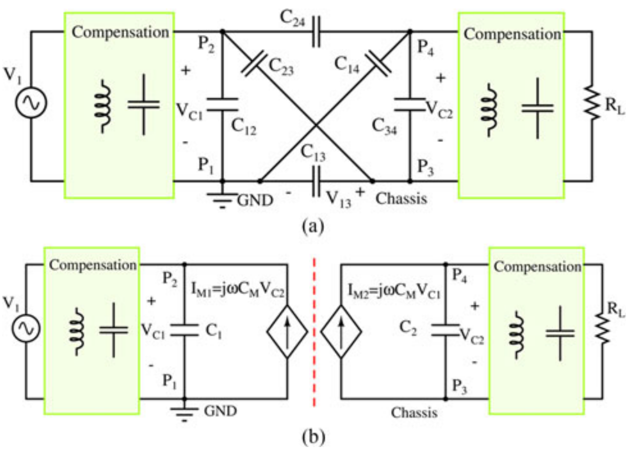

Fig. 2. Equivalent model of a two-plate CPT system with ground and chassis. (a) Six-capacitance model. (b) Behavior-source moel.

example, it can be buried into the ground to maintain a good connection. Then, as long as the connection with the ground is good enough, the size of the ground-side plate can be much smaller than the vehicle chassis. Since the ground-side plate directly connects with the compensation circuit, all the parasitic displacement currents from the chassis to the earth ground will be aggregated to this ground-side plates and then flow back into the compensation circuit.

B. Equivalent Circuit Model

In Fig. 1, the earth ground P_1, the vehicle chassis P_3, and the plates P_2 and P_4 work together as a capacitive coupler, which is represented by a six-capacitance and a behavior-source model [7], as shown in Fig. 2. The self-capacitances are defined as C_1 and C_2, and the mutual capacitance is defined as C_M, as shown below. The coupling coefficient is defined as $k_C = C_M/\sqrt{C_1 C_2}$:

$$\begin{cases} C_1 &= C_{12} + \dfrac{(C_{13}+C_{14})\cdot(C_{23}+C_{24})}{C_{13}+C_{14}+C_{23}+C_{24}} \\ C_2 &= C_{34} + \dfrac{(C_{13}+C_{23})\cdot(C_{14}+C_{24})}{C_{13}+C_{14}+C_{23}+C_{24}} \\ C_M &= \dfrac{C_{13}C_{24}-C_{14}C_{23}}{C_{13}+C_{14}+C_{23}+C_{24}} \end{cases}. \tag{1}$$

C. System Power Calculation

The behavior-source model in Fig. 2(b) is used to calculate system power. The load is represented by an equivalent resistance R_L. The voltage between P_2 and the ground is defined as V_{C1}, and the voltage between P_4 and the chassis is defined as V_{C2}. The voltage V_{C1} is chosen as the reference phasor, and the phase difference with V_{C2} is defined as θ, resulting in

$$V_{C2} = |V_{C2}| \cdot (\cos\theta + j\sin\theta). \tag{2}$$

According to Fig. 2(b), the apparent power absorbed by I_{M1} is defined as S_M and expressed as

$$\begin{aligned} S_M = P_M + jQ_M &= V_{C1}\cdot(-j\omega C_M V_{C2})^* \\ &= \omega C_M |V_{C1}|\cdot|V_{C2}|\cdot\sin\theta + j\omega C_M |V_{C1}|\cdot|V_{C2}|\cdot\cos\theta. \end{aligned} \tag{3}$$

Therefore, the active power P_M and reactive power Q_M are expressed as

$$\begin{cases} P_M &= \omega C_M |V_{C1}|\cdot|V_{C2}|\cdot\sin\theta \\ Q_M &= \omega C_M |V_{C1}|\cdot|V_{C2}|\cdot\cos\theta \end{cases}. \tag{4}$$

It shows that the system power is proportional to switching frequency ω, mutual capacitance C_M, voltage stresses $|V_{C1}|$, and $|V_{C2}|$, and also relates to the phase angle θ.

D. Voltage Stress

The six-capacitance model in Fig. 2(a) is used to calculate the chassis voltage V_{13}, which is expressed as

$$V_{13} = \frac{(C_{23}+C_{24})\cdot V_{C1} - (C_{14}+C_{24})\cdot V_{C2}}{C_{13}+C_{14}+C_{23}+C_{24}}. \tag{5}$$

Substituting (2) to (5), the magnitude of $|V_{13}|$ is expressed as

$$|V_{13}| = \frac{\sqrt{A^2+B^2-2A\cdot B\cdot\cos\theta}}{C_{13}+C_{14}+C_{23}+C_{24}} \tag{6}$$

where

$$\begin{cases} A = (C_{23}+C_{24})\cdot|V_{C1}| \\ B = (C_{14}+C_{24})\cdot|V_{C2}| \end{cases}. \tag{7}$$

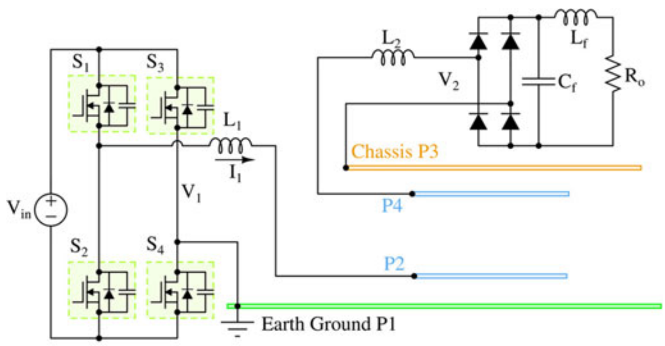

Fig. 3. Circuit topology of a two-plate CPT system.

Considering the power equation (4), if $|V_{C1}|$ and $|V_{C2}|$ satisfy

$$|V_{C1}| = \sqrt{\frac{C_{14}+C_{24}}{C_{23}+C_{24}}}\sqrt{\frac{P_M}{\omega C_M \sin\theta}},$$
$$|V_{C2}| = \sqrt{\frac{C_{23}+C_{24}}{C_{14}+C_{24}}}\sqrt{\frac{P_M}{\omega C_M \sin\theta}}. \tag{8}$$

$|V_{13}|$ can reach its minimal value, which is expressed as

$$|V_{13}|_{\min} = \frac{\sqrt{2\,(C_{23}+C_{24})\cdot(C_{14}+C_{24})}}{C_{13}+C_{14}+C_{23}+C_{24}}\cdot\sqrt{\frac{P_M}{\omega C_M}} \cdot\sqrt{\frac{1-\cos\theta}{\sin\theta}}. \tag{9}$$

In a capacitive coupler, the capacitances C_{14} and C_{23} are usually much smaller than C_{13} and C_{24} [7]. If the phase angle θ is much smaller than $\pi/2$, (8) and (9) can be simplified as

$$|V_{C1}| = |V_{C2}| \approx \sqrt{\frac{P_M}{\omega C_M \sin\theta}},$$
$$|V_{13}|_{\min} \approx \frac{C_{24}}{C_{13}+C_{24}}\cdot\sqrt{\frac{P_M}{\omega C_M}}\cdot\sqrt{\sin\theta}. \tag{10}$$

In the vehicle charging application, the chassis P_3 is much larger than the plate P_4, resulting in $C_{24} << C_{13}$. According to (1), C_M is approximately equal to C_{24}. Then, the voltage stresses are further simplified as

$$\begin{cases} |V_{C1}| = |V_{C2}| \approx \sqrt{\frac{P_M}{\omega C_{24}\sin\theta}} \\ |V_{13}|_{\min} \approx \frac{\sqrt{C_{24}}}{C_{13}}\cdot\sqrt{\frac{P_M}{\omega}}\cdot\sqrt{\sin\theta} \end{cases}. \tag{11}$$

According to (11), for a given system power P_M, there are three methods to reduce the chassis voltage $|V_{13}|$: increasing the switching frequency ω; designing the capacitive coupler structure to increase C_{13} and decrease C_{24}; and designing a compensation circuit to reduce $\sin\theta$. It needs to be noted that decreasing sinθ can increase the voltages $|V_{C1}|$ and $|V_{C2}|$.

E. Compensation Circuit Design

An example of the compensation circuit topology is shown in Fig. 3. A full-bridge inverter is used on the primary side to provide an ac excitation. A full-bridge rectifier and a low-pass filter ($L_f - C_f$) are used on the secondary to provide a dc current to the output resistor R_o. Two compensation inductors L_1 and L_2 are adopted on the primary and secondary sides, respectively, to resonate with the capacitive coupler. Using the fundamental harmonics approximation method and the coupler model in Fig. 2(b), it can be simplified as Fig. 4.

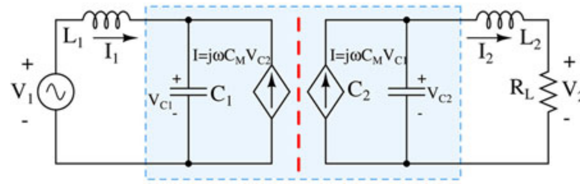

Fig. 4. Simplified circuit topology of a two-plate CPT system.

This circuit topology is similar to the double-sided *LC* compenation in [6], except that the external capacitances are eliminated and only an external inductor is required at each side. The equivalent resistance is expressed as $R_L = R_o \times 8/\pi^2$. The voltages V_{C1} and V_{C2} are expressed as

$$\begin{cases} V_{C1} = V_1 - I_1\cdot j\omega L_1 \\ V_{C2} = V_2 + I_2\cdot j\omega L_2 \end{cases}. \tag{12}$$

According to [6], the compensation inductors L_1 and L_2 can be designed to achieve a constant voltage working mode, resulting in

$$\begin{cases} L_1 = \frac{1}{1-k_C}\cdot\frac{1}{\omega^2 C_1} \\ L_2 = \frac{1}{1-k_C}\cdot\frac{1}{\omega^2 C_2} \end{cases}. \tag{13}$$

In Fig. 4, if the parameters are designed to be symmetric ($L_1 = L_2, C_1 = C_2, k_C = C_M/C_1$), the input current I_1 is calculated as

$$I_1 = \frac{V_1}{R_L}\cdot\left(1 - j\cdot\frac{C_1+C_M}{C_M}\cdot\frac{R_L}{\omega L_1}\right). \tag{14}$$

According to [6], at the constant voltage mode, the input voltage V_1 and output voltage V_2 have the same magnitude and 180° phase difference, which means $V_2 = -V_1$. Since a resistive load R_L is used at the output side, the output voltage V_2 is in phase with the output current I_2. Then, V_{C1} and V_{C2} can be rewritten as

$$\begin{cases} V_{C1} = -V_1\cdot\frac{C_1}{C_M} - V_1\cdot\frac{j\omega L_1}{R_L} = |V_{C1}|\angle\theta_1 \\ V_{C2} = -V_1 - V_1\cdot\frac{j\omega L_1}{R_L} = |V_{C2}|\angle\theta_2 \end{cases} \tag{15}$$

where θ_1 and θ_2 are the phases of V_{C1} and V_{C2}, and their phase difference is θ. If the parameters are designed to satisfy $\omega L_1 >> R_L\cdot C_1/C_M$, θ and sinθ can be approximated to be

$$\sin\theta \approx \theta \approx \frac{C_1}{C_M}\cdot\frac{R_L}{\omega L_1} - \frac{R_L}{\omega L_1} = \frac{R_L}{C_M}\cdot\frac{1}{\omega^2 L_1^2}. \tag{16}$$

It can be concluded that for a constant voltage the working mode *LC*-compensated CPT system, sinθ can be reduced through decreasing the load resistance R_L, increasing the coupling capacitance C_M, and increasing the compensation inductance L_1.

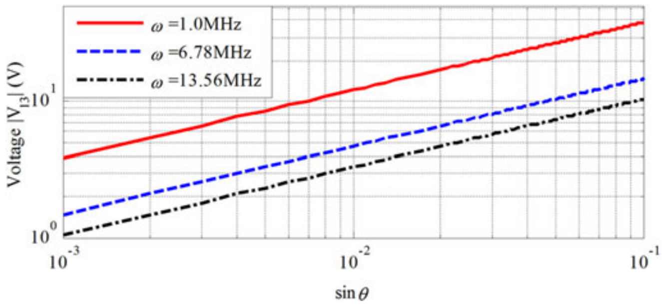

Fig. 5. Calculated voltage on chassis in a 3.0-kW two-plate compact CPT system.

III. Design Example

A. 3.0-kW Full Power Example

In a practical application as shown in Fig. 1, the chassis size of a passenger car is about 4.6 m × 1.8 m [10], which can be used to transfer 3.0-kW power. In this design, the size of plates P_2 and P_4 is chosen to be 0.45 m × 0.45 m, and their air-gap distance is set to be 110 mm. The finite element analysis by Maxwell shows that $C_{13} = 706$ pF and $C_{24} = 15.5$ pF. Then, $|V_{13}|$ can be calculated using (11), as shown in Fig. 5.

It shows that increasing the switching frequency ω and decreasing $\sin\theta$ both help to decrease voltage $|V_{13}|$. For example, if the system switches at 6.78 MHz, the chassis voltage can be limited to be lower than 8.35 V, as long as the compensation circuit is designed to maintain $\sin\theta$ lower than 0.03.

B. 350-W Downsized Prototype Design

Considering the space limitation in our lab, a 0.91 m × 0.91 m metal plate is used to act as the vehicle chassis. The size of plates P_2 and P_4 is also 0.45 m × 0.45 m, and the air-gap is 110 mm. To achieve similar power density as the previous 3.0-kW system, the power of this system is downscaled to be 350 W. On the primary side, a metal plate P_1 is also used and connected to the earth ground to reduce the conductive loss. The capacitances are measured as $C_{12} = 134$ pF, $C_{13} = 82$ pF, $C_{24} = 15$ pF, and $C_{34} = 124$ pF. Two inductors ($L_1 = 188$ μH, $L_2 = 20$ μH) are used on the primary and secondary sides [6]. Silicon carbide devices are used in the inverter and rectifier to provide 1-MHz switching frequency, and a 20-Ω resister is connected with the rectifier as the load. Then, the prototype is shown in Fig. 6.

In this experimental prototype, the bottom plate acts as the ground-side plate, and it is directly connected to the earth ground in the power socket on the wall with a wire. Therefore, the bottom plate has the same potential as the earth ground and becomes part of the earth ground. The capacitance between the top and bottom plate acts as the parasitic capacitance between the vehicle chassis and the earth ground, and the current flowing from the bottom plate back to the compensation circuit can be treated as the returning current from the earth ground.

The voltages on the plates and chassis can cause electric field emissions to the surrounding environment. In this 350-W CPT system, circuit simulation by LTspice shows that the voltage on

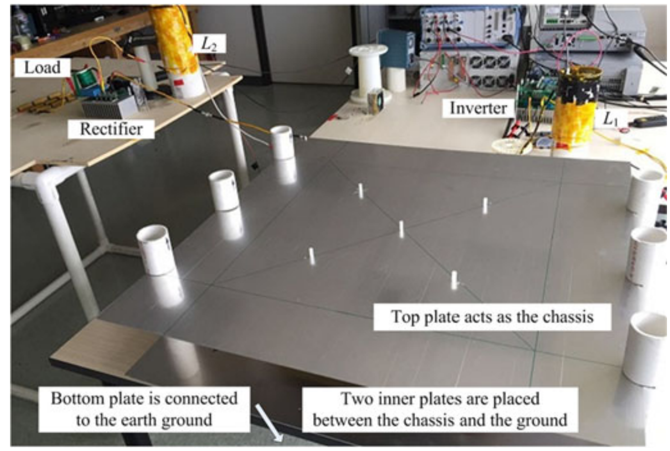

Fig. 6. Prototype of a downsized two-plate CPT system with a ground-side plate.

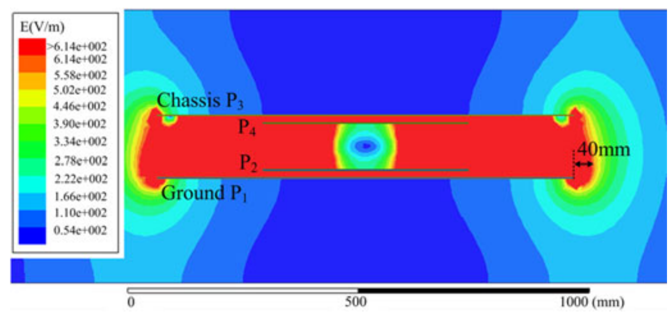

Fig. 7. Electric field emissions of a downsized two-plate CPT system.

plates P_2 and P_4 can be 7 kV, and the voltage on the chassis is about 130 V. Using these voltages as excitations, the electric field emissions are simulated using Maxwell as shown in Fig. 7.

The Maxwell simulation shows that most of the electric fields concentrate between the chassis and the earth ground, and the electric field emissions are limited. According to IEEE C95.1 standard [8], the human exposure of electric fields at 1 MHz should be lower than 614 V/m. The simulation result shows that the safe range of this two-plate system is 40 mm away from the edge of the coupler.

IV. Experimental Results

A. Well-Aligned Case

In the well-aligned case, as the input dc voltage reaches 100 V, the system achieves 356-W output power. The dc–dc efficiency from the dc source to the dc load including the power electronics circuit reaches 74.1%. The experimental waveforms are shown in Fig. 8, in which Fig. 8(a) indicates that a unity power factor is realized on both the input and output sides.

The chassis voltage was measured with its RMS value with respect to the ground at 132 V. Because of the parasitic capacitance of the voltage probe, the voltages V_{C1} and V_{C2} cannot be measured directly with the probe. Therefore, they should be measured by the indirect method. According to (12), using the measured waveforms of V_1, I_1, V_2, and I_2 from the oscilloscope, the waveforms of V_{C1} and V_{C2} can then be acquired and plot in

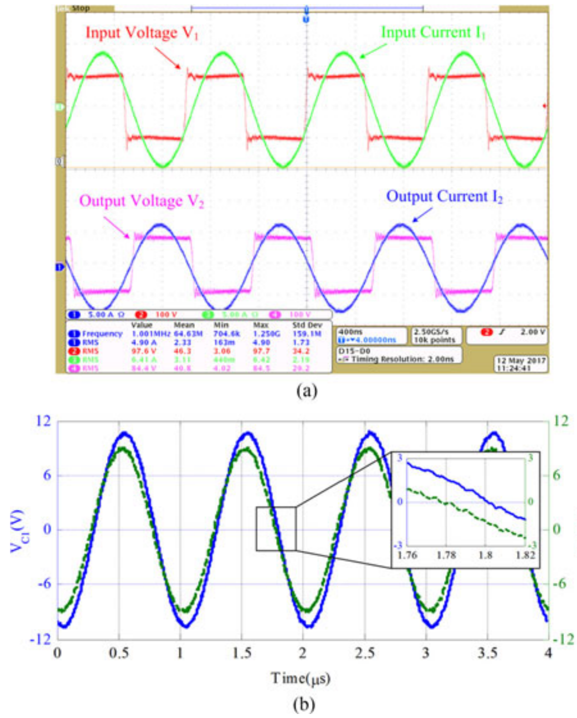

Fig. 8. Experimental waveforms of a downsized two-plate CPT system with a ground-side plate. (a) Input and output. (b) Plate voltage V_{C1} and V_{C2}.

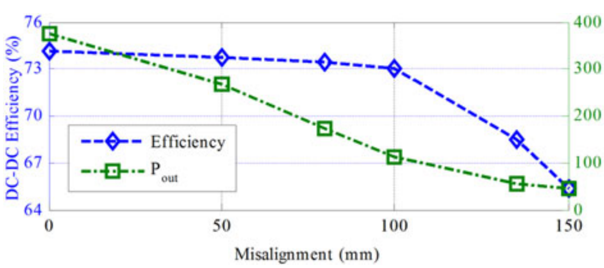

Fig. 9. Experimental output power and dc–dc efficiency in misalignment cases.

MATLAB, as shown in Fig. 8(b). It shows that the experimental RMS values of V_{C1} and V_{C2} are 7.5 and 6.5 kV, respectively, which agree with the simulation results. The enlarged figure shows the details which indicate that their time difference is about 0.22 μs, which is about 8° difference at 1 MHz, resulting in a sinθ of 0.14.

B. Misaligned Case

When there are misalignments, the coupling capacitances decrease and the resonances in the circuit are affected, resulting in the reduction of system power and efficiency. The system power and efficiency are measured in misalignment cases as shown in Fig. 9.

It shows that when the misalignment is 80 mm, the output power drops to 46% of the well-aligned value. When the misalignment is 150 mm, it drops to 12% of the well-aligned value. It also shows that the system efficiency decreases with the misalignment. With a misalignment of 80 mm, the dc–dc efficiency is 73.4%, and it reduces to 65.3% at 150-mm case.

In misalignment cases, since the resonances in the circuit are affected, it is very important to measure the chassis voltage and avoid the chassis voltage increase. The good news is that the experimental results indicate a decrease of chassis voltage with misalignment, which is acceptable. In our future research, the misalignment performance will be improved to maintain the system power and efficiency without increasing the chassis voltage.

C. Discussion: Impact of Ground-Side Plate on the Efficiency

The efficiency of the double-sided *LC*-compensated CPT system is expressed as

$$\eta_{LC} = \frac{I_{RL}^2 \cdot R_L}{I_{RL}^2 \cdot R_L + I_{L2}^2 \cdot R_{L2} + I_{C2}^2 \cdot R_{C2} + I_{C1}^2 \cdot R_{C1} + I_{L1}^2 \cdot R_{L1}} \tag{17}$$

where I_{C1}, I_{L1}, I_{C2}, I_{L2}, and I_{RL} are the currents flowing through the circuit components, and R_{C1}, R_{C2}, R_{L1}, and R_{L2} are their parasitic resistances. R_{C1} represents the ground-side resistance from the capacitive coupler to the compensation circuit.

According to Section II-E, the compensation parameters are designed to achieve a constant voltage working mode. If the circuit parameters are symmetric, using the parameter relationship in (13), the system efficiency can be simplified and expressed as

$$\eta_{LC} = \frac{1}{1 + \alpha_1 + \alpha_2 + \frac{1}{k_C^2 Q_1 Q_2} \cdot \left(\alpha_2 + \frac{1}{\alpha_2} + 2\right)} \tag{18}$$

where α_1 and α_2 are the resistance ratios, and Q_1 and Q_2 are the quality factors expressed as

$$\begin{cases} R_1 = R_{L1} + R_{C1}, R_2 = R_{L2} + R_{C2} \\ Q_1 = 1/(\omega C_1 R_1), Q_2 = 1/(\omega C_2 R_2) \\ \alpha_1 = R_1/R_L, \alpha_2 = R_2/R_L \end{cases} . \tag{19}$$

It shows that increasing the ground-side resistance R_{C1} can increase the primary resistance ratio α_1, which leads to a decrease of the system efficiency. Therefore, as shown in Fig. 6, a metal plate can be used at the ground side to reduce R_{C1} and improve the system efficiency. In a real application, depending on the conductivity of the earth ground, this plate can be reduced or even eliminated.

In our lab, the floor is made by concrete containing iron bars. Since the connections between the iron bars and the earth ground are not well maintained, the conductivity of the floor is not comparable with a piece of aluminum plate. The capacitive coupler is placed on the floor without the ground-side plate, and the other plates have the same dimensions. The compensation inductors L_1 and L_2 are also the same. The capacitance between the plate P_2 and the earth ground is about 60 pF, which requires an external capacitor C_{ex1} (74 pF) connecting in parallel with P_2 and the earth ground to establish the circuit resonance.

The measured waveforms are similar to those in Fig. 8(a). Since the ground-side resistance is increased, the power loss is increased. When the input dc voltage reaches 100 V, the system reaches 116.8-W output power with 40.3% dc–dc efficiency.

It should be pointed out that this is the worst case, because the ground-side plate is completely eliminated and the conductivity of the earth ground is not optimized. But it can provide the guideline to improve the system performance in future application.

V. Conclusion

This letter proposes a two-plate compact CPT system for electric vehicle charging applications. The vehicle chassis and the earth ground are exploited to transfer power, which can simplify the structure of the CPT system. The voltage on the vehicle chassis is studied, which provides three methods to reduce the chassis voltage for safe operation. A 3.0-kW two-plate CPT system is designed for an electric vehicle. When the switching frequency is 6.78 MHz and the compensation circuit is well designed, the chassis voltage can be limited to 8.35 V, which is safe for humans. Also, a downsized 350-W downsized prototype is implemented with a 132-V chassis voltage. In the future prototype design, the switching frequency will be increased and the compensation circuit will be improved to further reduce the chassis voltage.

References

[1] Y. Su *et al.*, "A capacitive power transfer system with a mixed-resonant topology for constant-current multiple-pickup applications," *IEEE Trans. Power Electron.*, vol. 32, no. 11, pp. 8778–8786, Nov. 2017.

[2] S. Li, Z. Liu, L. Zhu, C. Shuai, and Z. Chen, "Wireless power transfer by electric field resonance and its application in dynamic charging," *IEEE Trans. Ind. Electron.*, vol. 63, no. 10, pp. 6602–6612, Oct. 2016.

[3] L. Huang, A. P. Hu, A. K. Swain, and Y. Su, "Z-impedance compensation for wireless power transfer based on electric field," *IEEE Trans. Power Electron.*, vol. 31, no. 11, pp. 7556–7563, Nov. 2016.

[4] F. Lu, H. Zhang, H. Hofmann, and C. Mi, "A double-sided LCLC-compensated capacitive power transfer system for electric vehicle charging," *IEEE Trans. Power Electron.*, vol. 30, no. 11, pp. 6011–6014, Nov. 2015.

[5] L. Huang, A. P. Hu, A. Swain, and X. Dai, "Comparison of two high frequency converters for capacitive power transfer," in *Proc. IEEE Energy Conv. Cong. Exp.*, 2014, pp. 5437–5443.

[6] F. Lu, H. Zhang, H. Hofmann, and C. Mi, "A double-sided LC compensation circuit for loosely-coupled capacitive power transfer," *IEEE Trans. Power Electron.*, 2017. doi: 10.1109/TPEL.2017.2674688.

[7] H. Zhang, F. Lu, H. Hofmann, W. Liu, and C. Mi, "A four-plate compact capacitive coupler design and LCL-compensated topology for capacitive power transfer in electric vehicle charging application," *IEEE Trans. Power Electron.*, vol. 31, no. 12, pp. 8541–8551, Dec. 2016.

[8] *IEEE Standard for Safety Levels with Respect to Human Exposure to Radio Frequency Electromagnetic Fields, 3kHz to 300 GHz, C95.1*, 2005.

[9] International Electrotechnical Commission, *Method of Measurement of Touch Current and Protective Conductor Current*, IEC 60990, 1999.

[10] 2016. [Online]. Available: http://automobiles.honda.com/2016/civic-sedan/specifications.aspx